# CHAPTER V

# FACILE SYNTHESIS OF FLOWER-LIKE BISMUTH OXIDE: CONTROLLABLE MORPHOLOGY

## 5.1 Abstract

Flower-like bismuth oxide is successfully synthesized via a facile route, based on thermal decomposition of the precursor obtained by heating bismuth nitrate pentahydrate in ethylene glycol solution with and without triethanolamine (TEA) at 100°–200 °C for 2 h. The precursor is characterized using Fourier transform infrared spectroscopy (FT-IR), Thermogravimetric-differential thermal analysis (TG-DTA), X-ray diffraction (XRD), and Field emission scanning electron microscopy (FE-SEM). The influences of reaction temperature, TEA, and metal concentration are investigated. At temperatures as low as 100 °C,TEA can not only catalyze the reaction, but also affect the nanostructure formation. In the absence of TEA and by adjusting the bismuth ion concentration, different types of the flower-like structure are obtained. After calcinations at 300°–500 °C, the flower-like bismuth oxide is still maintained.

## 5.2 Introduction

Bismuth oxide is widely used in a number of applications, such as solid oxide fuel cells,[1] sensors[2] and opto-electronics[3]. It has been especially considered as a potential photocatalyst under visible light due to its wide energy gap, around 2.0–3.96 eV.[4-5] In the past few years, various morphologies of bismuth oxide—such as hand-like[6], mesh-like,[7] prism-like,[8] shuttle with concave surface,[9] or flower-like structure—have been reported.[10] Many efforts have been made to control the growth and the morphology of bismuth oxide nanostructure formation. For example, Zhang *et al.*[11] reported the template-free process for fabrication of flower-shaped $Bi_2O_3$ by dissolving bismuth nitrate in nitric solution and using citric acid as a

capping agent.[11] Using a similar template-free aqueous method, Zhou *et al.* introduced $VO_3^-$ into the reaction system while keeping the pH solution at 12 and obtained uniform hierarchical nanostructures of $Bi_2O_3$.[12] Tseng *et al.* successfully synthesized flower-like bismuth oxide in nitric acid with the aid of polyethylene glycol-8000 (PEG-8000) as a capping agent[13] while Geng *et al.* also prepared a flower-like structure of $Bi_2O_3$ in nitric solution media using ice-water bath in the presence of polyvinyl alcohol[14]. However, the methods of both Tseng *et al.* and Geng *et al.* also required the addition of strong base (NaOH) into the mixture to before achieving the flower-like structure.

Herein, we report a facile route to synthesize flower-like bismuth oxide with controllable morphology and capability to scale-up for a large scale preparation, using alkoxide precursor synthesized from a simple route by heating bismuth nitrate in EG without adjusting pH and adding other chemical templates. Different characteristics of the flower-like structure were also studied.

## 5.3 Experimental

### 5.3.1 Bismuth Oxide Precursor Synthesis

Bismuth nitrate pentahydrate $Bi(NO_3)_3.5H_2O$, ≥98% purity, Fluka) was mixed with and without triethanolamine (TEA, 98% purity, QRëC) in 100 mL of ethylene glycol (EG, 99.9% purity, J.T.Baker). The mixture was carried out in a 250-ml three-necked round-bottom flask and placed in the oil bath. Then, it was stirred vigorously and heated under nitrogen atmosphere at various temperatures (100, 150, and 200 °C) to obtain precipitate. The precipitated powder was removed and washed with acetonitrile (99.9% purity, Lab-scan) several times to remove all $Bi(NO_3)_3.5H_2O$, TEA, and EG. The powder was then dried in vacuum desiccators at room temperature before calcinations at temperatures ranging from 300–500°C for 1 h using a heating rate of 0.5 °C/min to achieve bismuth oxide.

5.3.2 Characterization

FE-SEM (SEM; Hitachi/S-4800) was used to observe the morphological appearance of the bismuth glycolate precursor. FT-IR spectra (Nicolet iS10: FT-IR spectrometer) was used to investigate the chemical structure of organic functionality with a spectral resolution of 4 $cm^{-1}$, using transparent KBr pellets. TG-DTA was carried out using a Perkin Elmer thermal analysis system with a heating rate of 10 °C.$min^{-1}$ over a temperature range of 30–750°C to determine its thermal property. The surface area of all samples was measured using Quantachrom (Model Autosorp-1) surface area analyzer. The crystalline structure of the samples was analyzed on a Rigaku X-ray diffractometer system (RINT-2200) with a Cu tube for generating $CuK_\alpha$ radiation (1.5406 Å) and a nickel filter, a generator voltage of 40 kV, and a generator current of 30 mA. The scan speed of 5° (2θ)/min with a scan step of 0.02 (2θ) was used for a continuous run in a 5° to 60° (2θ) range.

## 5.4 Results and Discussion

5.4.1 Morphology and Structure of Bismuth Oxide Precursor

*5.4.1.1 Influence of Temperature*

To investigate the temperature effect, $Bi(NO_3)_3.5H_2O$ was heated in EG at different temperatures (100, 150, and 200 °C) using TEA as a catalyst to result in bismuth oxide precursor. FE-SEM results of the precursor are shown in Figure 1. The plate-like morphology with strong agglomerate was obtained at 100 °C synthesis temperature, as seen in Figure 1a, whereas a mixture of close-packed flower-like sphere with a diameter of 6–10 μm and spherical particles (Figure 1b) was observed at the higher temperature of 150 °C. The individual flower-like sphere taken at higher magnification is shown in the inset of this figure. When increasing the temperature to 200 °C (Figure 1c), the close-packed flower-like sphere was larger in size (around 10–15 μm).When the surface of the sphere was closely observed, it was found that there were small particles between nanosheets.

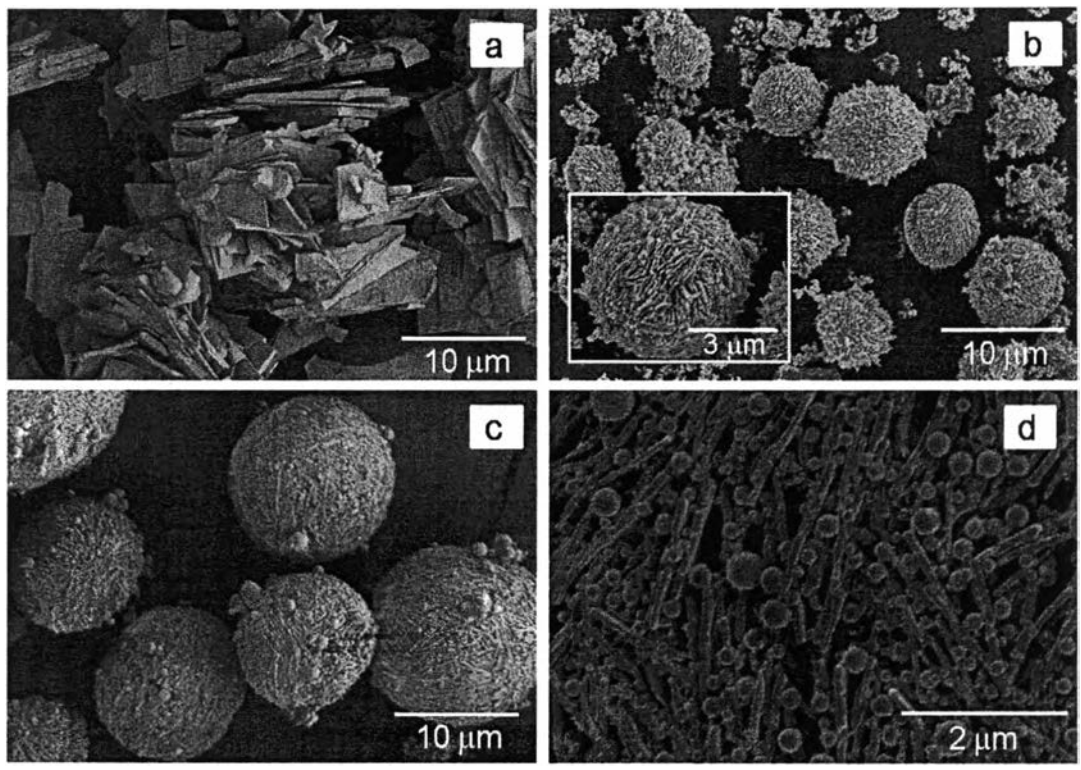


**Figure 5.1** Morphology of bismuth oxide precursor synthesized at; a) 100°, b) 150°, and c-d) 200 °C.

Heating metal oxide or metal salts in polyol medium usually leads to the formation of glycolate precursors.[15-17] Thus, in our case, to confirm the structure, the FT-IR spectra of EG and precursors obtained from heating at different temperatures were determined, as shown in Figure 2. The following functional groups were detected; -OH stretching (3200–3500 $cm^{-1}$), C-H stretching (1460–1380), C-O symmetric stretching (1089–1038 $cm^{-1}$), C-H stretching (866 $cm^{-1}$), and C-O-H bending (640 $cm^{-1}$). FT-IR spectra of all precursors showed peak at 1384 $cm^{-1}$, referring to N-O symmetric stretching of free $NO_3^-$.[18] Absorption band at 580 $cm^{-1}$ corresponds to Bi-OR stretching of bismuth ethylene glycolate.[19] It can be stated that the obtained precursor was bismuth glycolate precursor. It is worth noting that at higher synthesis temperatures (150 ° and 200 °C), the peak at 1089–1038$cm^{-1}$ increased, indicating more formation of the C-O bond. The peak at 1600 $cm^{-1}$ for the precursor obtained from 150 °C synthesis temperature belongs to bending vibration

of $H_2O$ adsorbed on the surface of the precursor.[20] However, this peak did not appear in the precursor synthesized at 200 °C due to a temperature that was extremely higher than the boiling point of water.

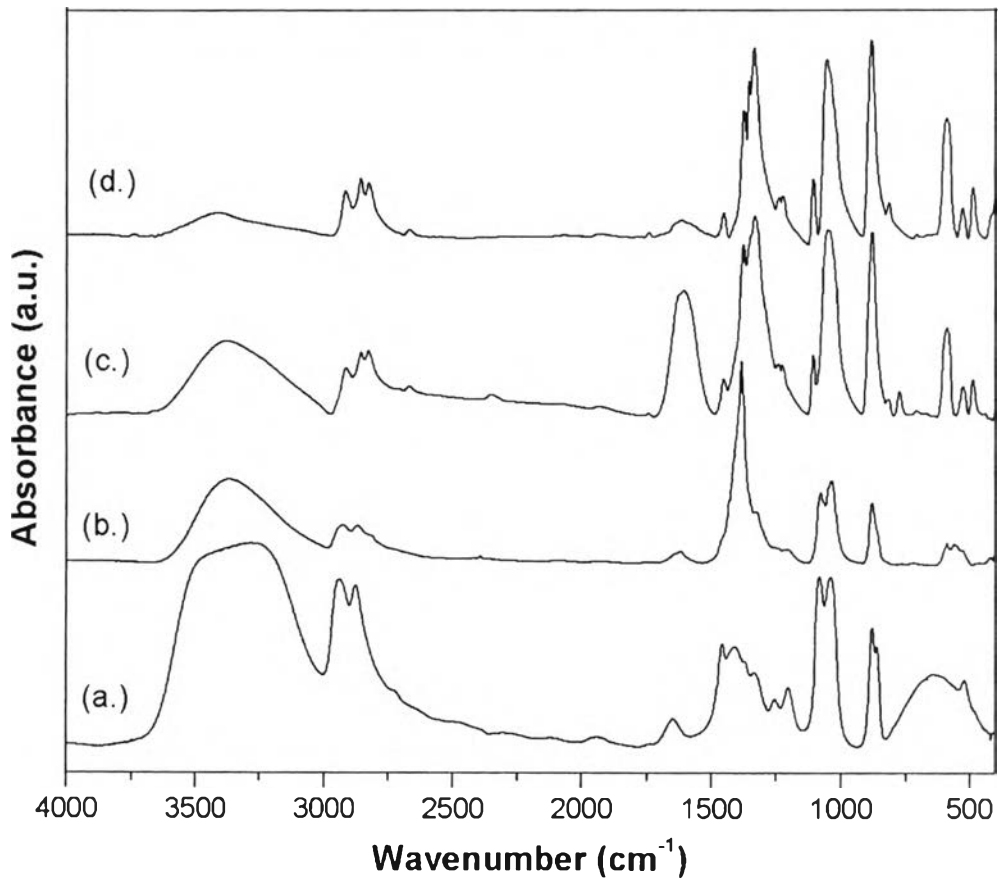


**Figure 5.2** FT-IR spectra of a) EG, and bismuth oxide precursor synthesized at b) 100°,c) 150°, and (d) 200 °C.

XRD patterns of all samples are presented in Figure 3. All of the bismuth oxide precursors mainly exhibit strong low angles, representing a highly crystalline phase. Although it lacks the XRD pattern information for metal alkoxides obtained in polyol media, such as EG, our results are similar to other transition glycolates, such as cobalt,[21] manganese or lithium[22] which also showed the highest intensity at low angle around ca. 10–11 2theta degree. These structures are described as stacked metal oxygen sheet intercalated with ethylene glycol. [23] The strong peak at

two theta degree of 10.78 of bismuth glycolate powder synthesized at 100 °C was slightly shifted to a higher angle at 11.62 and 11.64 for 150° and 200 °C, respectively. Interestingly, according to JCPDS 5-519, the XRD pattern of the sample synthesized at 200°C, showed the characteristic peaks of elemental bismuth.

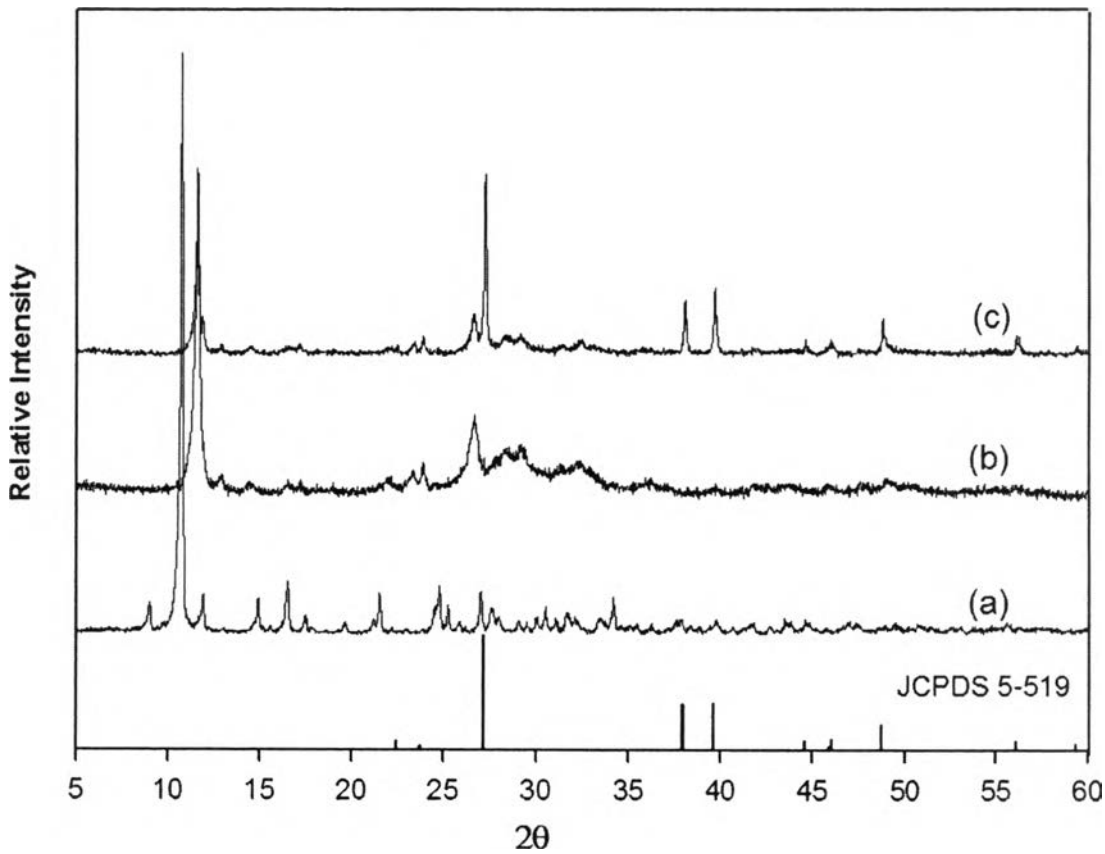


**Figure 5.3** XRD patterns of the bismuth oxide precursor synthesized at a) 100°, b) 150°, c) 200 °C, and JCPDS 5-519.

Undoubtedly, EG has an ability to reduce bismuth ion into elemental bismuth, and this ability increases with temperature and reaches the maximum value at its boiling point (ca. 198 °C).[15,23] In this so-called polyol process, the redox reaction of metallic compound occurred by accepting electrons from the oxidation of EG. When the hydroxyl groups are converted to carboxyl groups, the electrons and protons were released. This method is well known for preparation of

metal powder, such as Ag and Au.[24] Recently, Liu *et al.* prepared bismuth nanotube arrays by heating bismuth oxide in EG at 200 °C [25] and Goia *et al.* reported the preparation of colloidal bismuth particles in polyol.[26] Some parts of their investigation stated that when they heated bismuth salts (bismuth oxide) in polyol media at its boiling point, the bismuth glycolate platelets were slowly converted into elemental bismuth. The chemical reactions were proposed as follows;

$$HOCH_2CH_2OH \rightarrow CH_3CHO + H_2O \quad (1)$$

$$6CH_3\text{-}CHO + 2Bi^{3+} \rightarrow 3CH_3\text{-}CO\text{-}OC\text{-}CH_3 + 2Bi + 6H+ \quad (2)$$

When the reaction temperature reached 200 °C, causing EG to reach its maximum reducibility, some parts of bismuth glycolate were reduced to elemental bismuth. Therefore, to prevent the reduction of bismuth glycolate to elemental bismuth, the reaction temperature in this study was limited at 150 °C.

#### *5.4.1.2 Influence of TEA on nanostructure formation*

In this study, TEA was used to catalyze the reaction. At 100 °C temperature the reaction was first carried out with and without TEA. It was found that with TEA (0.1 mole) the reaction provided white powder of the precursor within 2 h whereas without TEA the precursor precipitate was obtained after 5 h. However, TEA had no effect on the reaction time when heating the reaction at 150 °C. In terms of nanostructure formation, different morphologies of the precursors were obtained from the reaction without TEA at 100° and 150 °C, as seen in Figure 4. Figures 4a-b show hexagonal plate-like structures of the bismuth oxide precursor synthesized at 100 °C. The thickness of each plate was in the range of 0.20–1.2 μm. At 150 °C, the flower-like spheres (Figures 4 c-d), consisting of nanosheets with a thickness around 60 nm, were obtained. Comparing the morphology of the precursors obtained with and without TEA in Figure 5, the nanoparticles still remained in the presence of 0.1 mole of TEA but disappeared in the absence of this catalyst. Thus, it could be proposed that TEA might have an effect on the hierarchical formation. To verify this point, a higher concentration of TEA (0.2 mol) was added to the $Bi(NO_3)_3.5H_2O$ and EG solution and the reaction was run at 150 °C. The results shown in Figure 5 illustrate the images of the bismuth oxide precursor synthesized without TEA

(Figures 5a-b), and with 0.1 and 0.2 mole of TEA (Figures 5 b-c and c-d, respectively). Without the catalyst, the flower-like size was larger than the precursor obtained from 0.1 mole of TEA. At the higher content of catalyst, the flower-like structure was transformed to a two-dimensional plate-like structure. Evidently, it supports the above assumption that TEA inhibited the flower-like formation. As a result, TEA was used as a catalyst for only the reaction run at low temperature (100 °C) and was unnecessary for high temperature (150 °C) since it significantly inhibited the flower-like formation. Thus, the flower-like bismuth oxide can be easily synthesized by only heating the bismuth nitrate in EG at 150 °C without adding other chemical compounds.

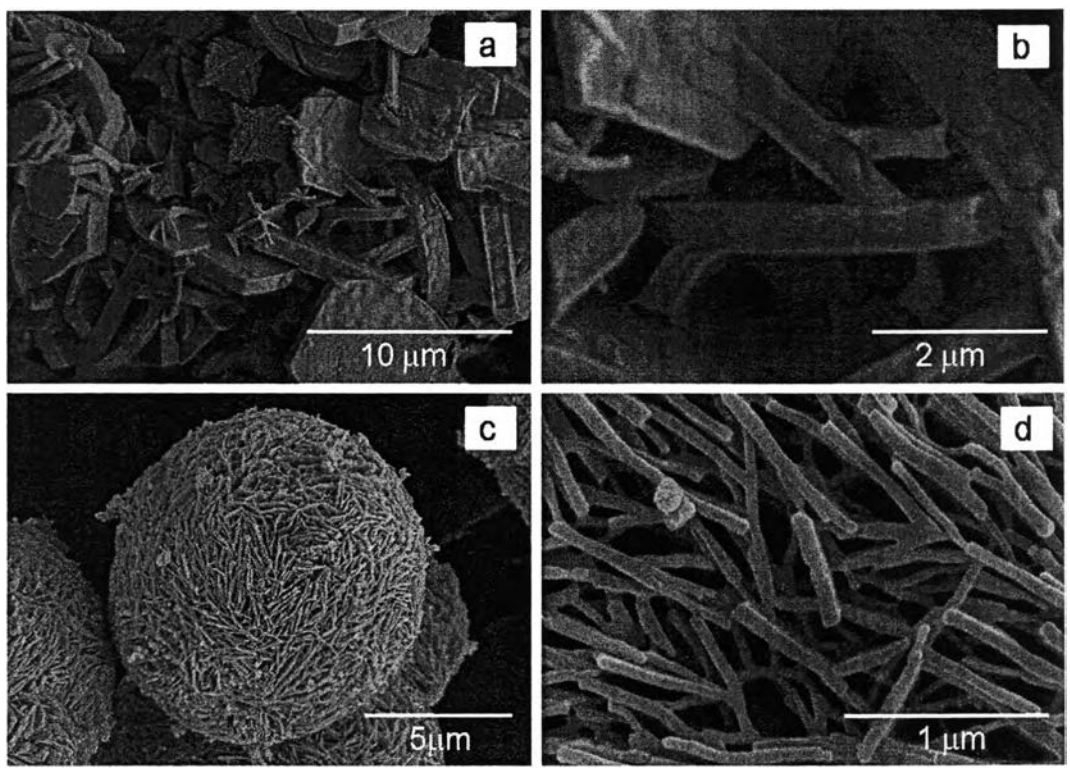


**Figure 5.4** Low and high magnifications of SEM images of the bismuth oxide precursor synthesized without TEA at temperature of a-b) 100°, and c-d) 150 °C

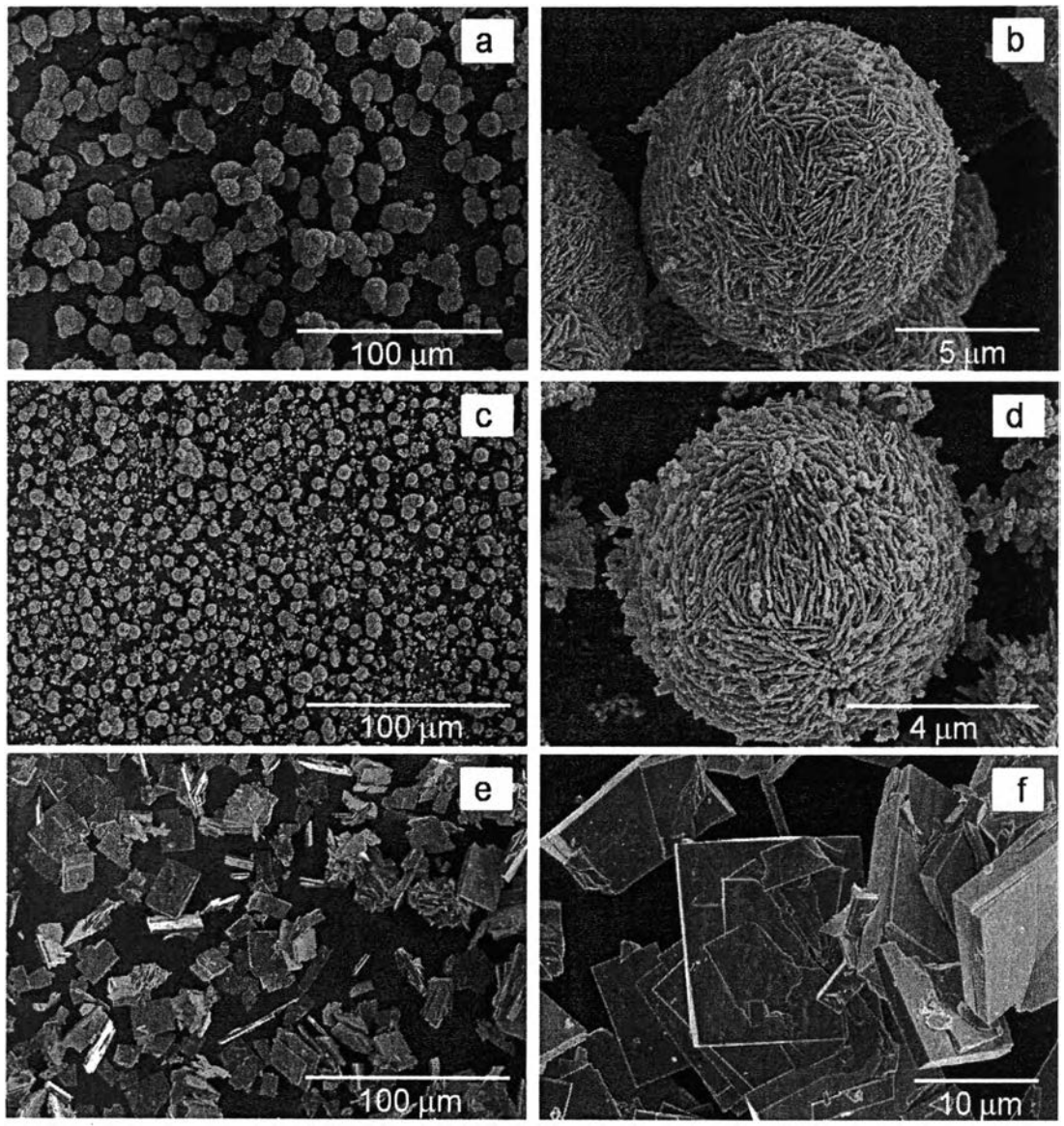


**Figure 5.5** Low and high magnifications of SEM images of the samples synthesized at 150 °C without TEA a-b), and with 0.1 (c,d), and 0.2 (e,f) mole of TEA.

*5.4.1.3 Morphology Evaluation*

The morphology evaluation of bismuth oxide precursor was investigated by carrying out a time-dependent reaction in which the samples were collected at intervals. The results in Figure 6 clearly show that at 5 min reaction time (Figure 6a), the bismuth oxide precursors were formed as spherical particles having

sizes around 50–80 nm. Prolonging the time to 15 min (Figure 6b) caused flower-like spheres to rapidly occur although the structure in this stage was not complete, as recognized from the remaining of nanoparticles. Figures 6c and d, presenting the morphologies of the precursors obtained after heating for 1 and 2 h, respectively, show the nearly full growth of the flower-like spheres, especially when the reaction reached 2h.

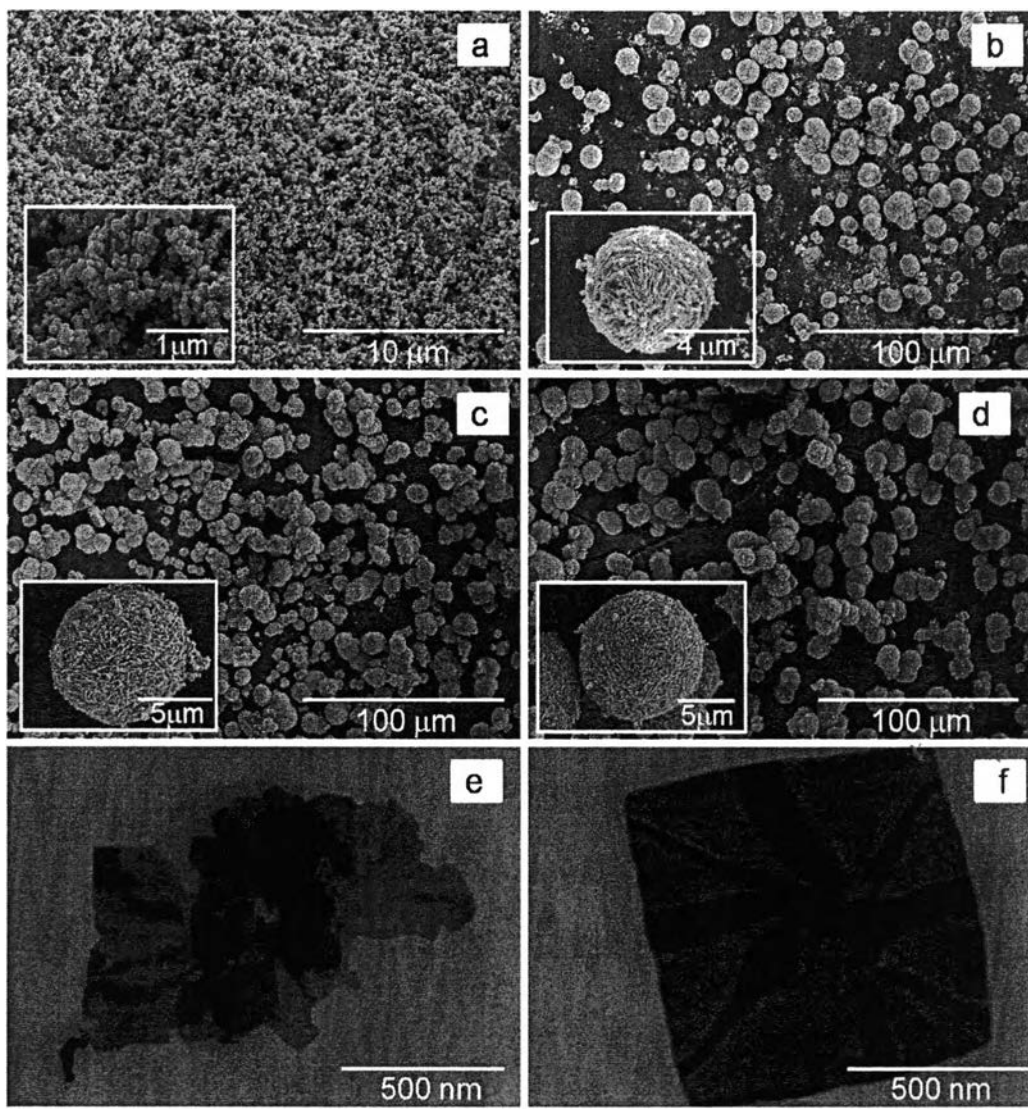


**Figure 5.6** Formation mechanism of the bismuth oxide flower-like structure obtained a) at 5 min, b) 15 min, c) 1h, d) 2h, e) STEM image of the bismuth oxide precursor synthesized for 2h without TEA (taken at 80,000 magnification), and f) STEM image of the individual nanoplate (taken at 90,000 magnification).

These results are consistent with the previous reports, explaining a fast nucleation of primary particles, followed by a slow aggregation and crystallization of the primary particles.[27-29] Similarly, in our study, the bismuth oxide precursor nuclei were quickly formed by coordination of bismuth ion and EG within the first 5 min and rapidly precipitated out from the solution. The nuclei (50–80 nm) then grew into nanoplates and the nanoplates arranged themselves into a flower-like structure through self assembly process. Ethylene glycol not only acted as solvent but it also facilitated the self assembly, as proposed by Yang *et al.* on a functionality of EG on the formation of 3D flower-like $Lu_2O_3$.[30] They explained that the nuclei of lutetium oxide precursor seeds were first formed through a homogeneous nucleation process, and subsequently recrystallized to grow into nanoflakes. In the presence of EG, acting as surfactant, the EG could be absorbed onto the flakes, leading to the self-assembly process. We further and more closely examined the precursor obtained from 2 h reaction time by low-voltage scanning transmission electron microscopy (STEM), see Figure 6c, and found the aggregation of two nanoplates, while Figure 6d illustrates the anisotropic growth of an individual plate.

#### *5.4.1.4 Influence of Metal Concentration*

The influence of metal concentration was also studied by varying the bismuth ion concentration from 25 mM to 150 mM without the use ofTEA. As can be seen by the results in Figure 7, the structure of the bismuth oxide precursor at 25 mM concentration (Figure 7a) has a semiconcave structure, composed of small petal plates attached from face-to-face attraction. The small plates attached layer by layer, which tended to curve into a circular shape. At concentrations as high as 50 mM, the flower-like structure was formed through the self-assembly of nanoplates, as seen in Figure 7b. The thickness of each plate is around 150–230 nm. When the concentration was increased to 100 mM (Figure7c), the flower-like structure composed of thinner plates appeared around 60 nm, and these plates arranged themselves in closed packs. At 150 mM concentration (Figure 7d), a mixture of small particles and the flower-like structure was observed. The plates assembled themselves loosely, as demonstrated in the inset of Figure 7d.

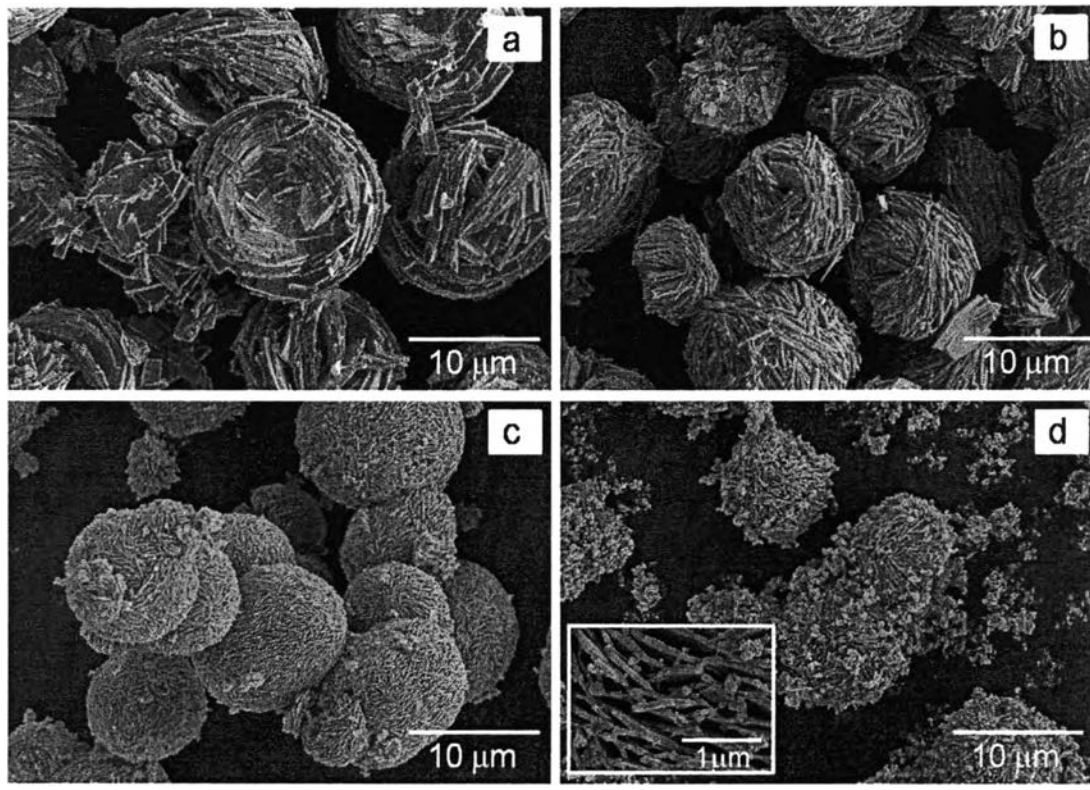


**Figure 5.7** SEM images of the samples using different initial concentrations of bismuth ion of a) 25mM, b) 50 M, c) 100 mM, and d) 150 mM.

Previous researches reported that the influence of metal ion concentration on the final morphology involved a hybrid mechanism of the crystal growth.[31-32] At low concentration, a limited number of nuclei led to the growth of a large plate with a curved structure. At medium concentration of 50 mM, the nuclei grew and formed anisotropic plates in which individual plates had more time to grow, causing thicker plates (150–230 nm). When the concentration reached 100 mM, higher numbers of nuclei presented in the solution, making the crystal grow faster and develop into a hierarchical self-assembled structure, resulting in the flower-like structure. However, too much nuclei in the solution only caused primary particles along with flower-like structure since these particles had not enough time to arrange further. The schematic diagram of the proposed growth mechanism of the flower-like structure of the bismuth oxide precursor is shown in Figure 8, and the

synthesis conditions, giving different morphologies of the bismuth oxide precursor, are summarized in Table 1.

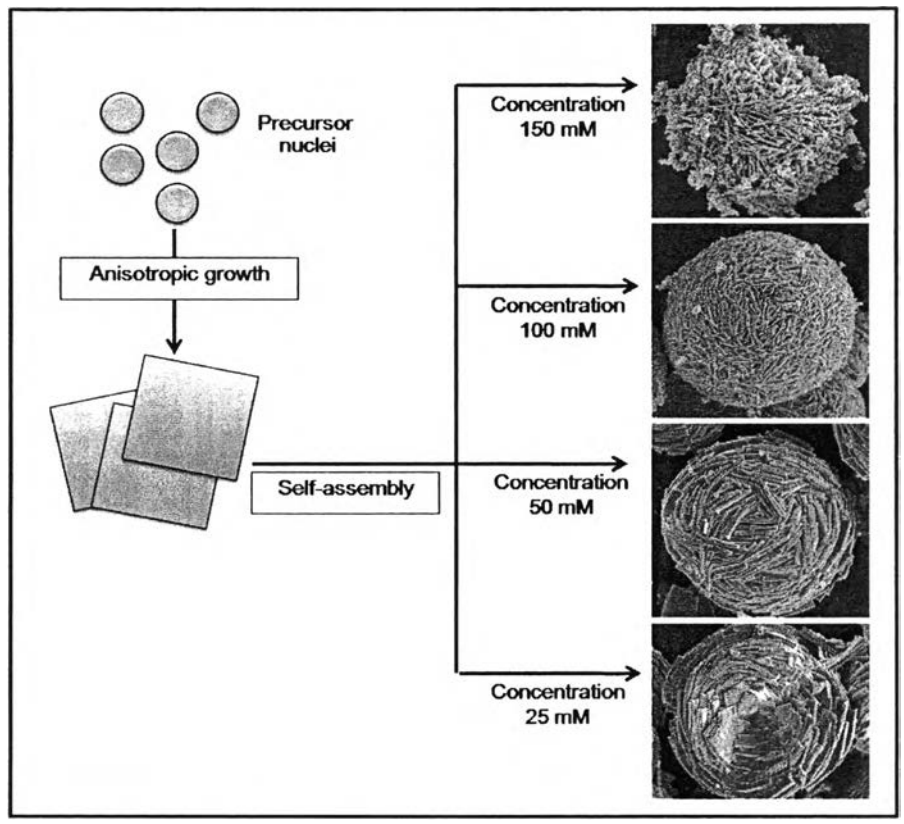


**Figure 5.8** Schematic diagram of the proposed growth mechanism of the flower-like structure of the bismuth oxide precursor.

**Table 5.1** Summarized synthesis conditions and morphologies of the bismuth oxide precursor.

| Sample | Synthesis condition | | | Morphology |
|---|---|---|---|---|
| | Temperature (°C) | Triethanolamine Concentration (mole) | Bismuth ion concentration (mmol) | |
| B1 | 100 | 1 | 100 | Plate like |
| B2 | 150 | 1 | 100 | Flower like (diameter 5-10 μm) and nanoparticles |
| B3 | 200 | 1 | 100 | Flower like (diameter 10-15 μm) |
| B4 | 150 | - | 100 | Flower like |
| B5 | 150 | 2 | 100 | Plate like |
| B6 | 150 | - | 25 | Semiconcave sphere |
| B7 | 150 | - | 50 | Flower like |
| B8 | 150 | - | 150 | Flower like and nanoparticles |

5.4.2 Bismuth Oxide Preparation and Characterization

Generally, polymorph bismuth oxide has mainly four crystalline phases: monoclinic ($\alpha$-$Bi_2O_3$), tetragonal ($\beta$-$Bi_2O_3$), faced center cubic ($\delta$-$Bi_2O_3$), and body center cubic ($\gamma$-$Bi_2O_3$).The monoclinic phase is stable at low temperature while the faced center cubic phase is high-temperature stable. The morphology and the crystalline phase of the bismuth oxide powder rather depend on synthesis route. For example, Yang *et al.* obtained $\beta$-$Bi_2O_3$ nanotubes by oxidizing metallic bismuth in air at 200–220°C.[33] In this study, thermal decomposition of the bismuth oxide precursor was measured to estimate calcinations temperature using TGA (Figure 9a). It was found that the maximum weight loss at 268 °C was around 33% assigned to the decomposition of chelating ethylene glycol. [34] Thus, the calcinations process was

started at 300 °C to insure that the precursor was completely transformed to the bismuth oxide.

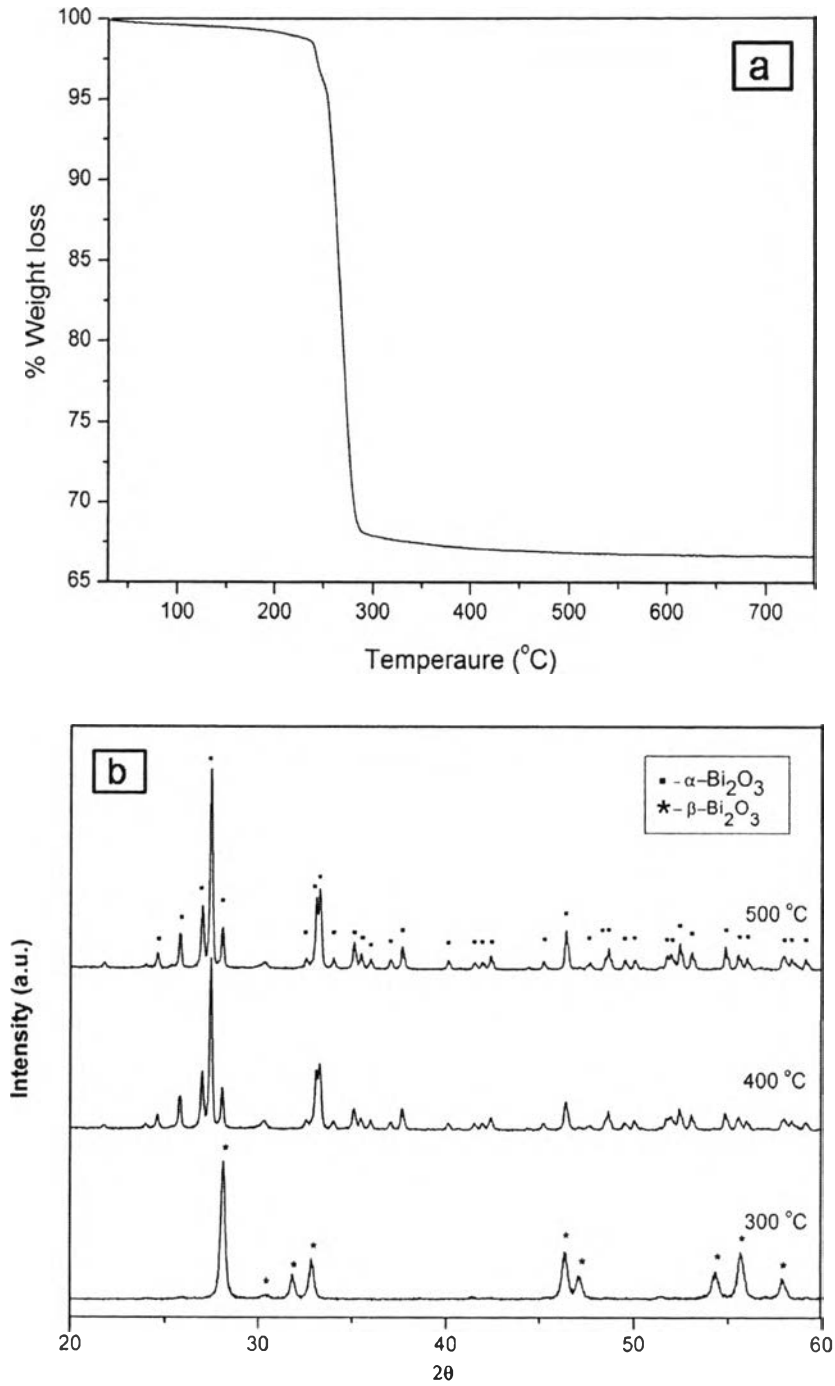


**Figure 5.9** a) TG-curve of the bismuth oxide precursor synthesized at 150 °C without TEA, and b) XRD patterns of the bismuth oxide obtained from calcining the bismuth oxide precursor at different temperatures.

The precursor was calcined at a temperature range of 300–500 °C for 1h using a heating rate of 0.5 °C/min, and the results were analyzed using XRD, as shown in Figure 9b. At 300 °C, we received a mixture of monoclinic and tetragonal phases whereas at higher temperatures, the tetragonal phase was transformed to monoclinic phase ($\alpha$-$Bi_2O_3$) and then to monoclinic single phase (PDF card No. 41-1449). The results of this work are similar to the work done by Monnerau *et al.* who obtained the tetragonal phase ($\beta$-$Bi_2O_3$) by decomposition of bismuth oxalate at a temperature range of 250–300 °C. The tetragonal phase is also stable up to 300 °C, which is the transition temperature to monoclinic phase.[35] The morphology of the bismuth oxide obtained from calcination at 300°–500 °C was illustrated in Figure 10. Figures 10a-b show the morphology of the bismuth oxide calcined at 300 °C and taken at low and high magnifications, respectively. The high magnification image indicates that each plate is composed of many nanoparticles.

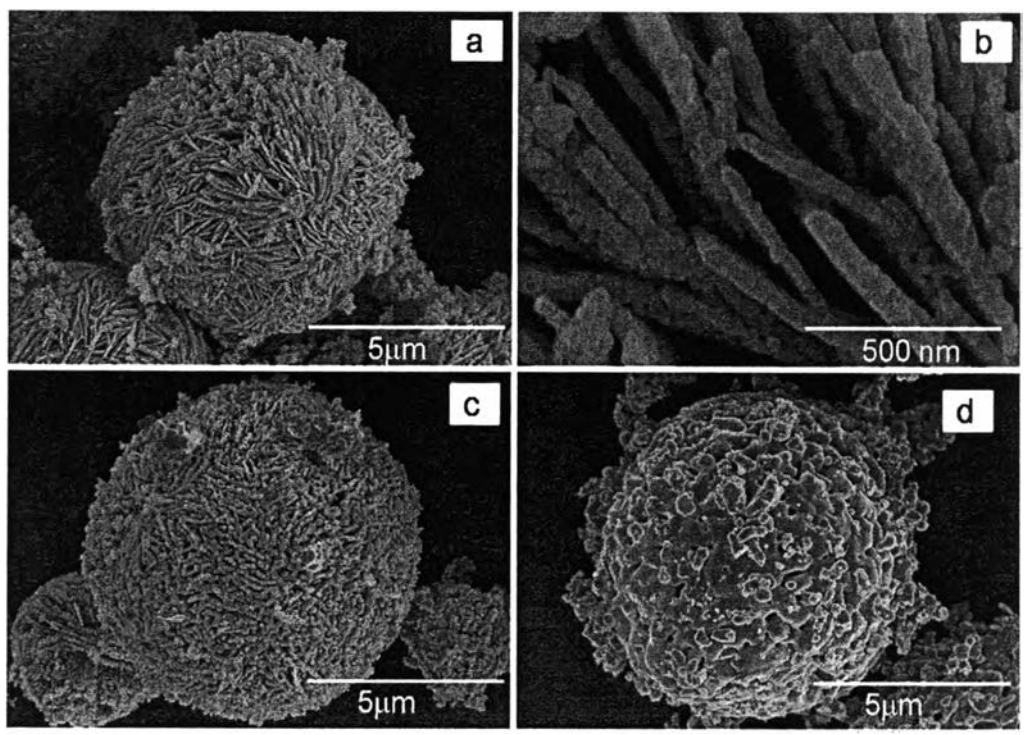


**Figure 5.10** SEM images of the bismuth oxide; a) calcined at 300 °C for 1h and taken at low magnification, and b) high magnification, c-d) calcined at 400 ° and 500 °C, respectively.

Figures 10c-d illustrate the morphologies of the bismuth oxide calcined at 400° and 500 °C, respectively. As we can see, the flower-like structure is still maintained in the bismuth oxide product. The Brunauer-Emmett-Teller (BET) surface areas of all calcinations products are summarized in Table 2. The thick wall (B7C300) and the thin wall flower-like (B4C300) bismuth oxides calcined at 300 °C had a very close surface area whereas the plate-like structure had lower surface area, 12.1 $m^2/g$. The surface areas even decreased further to 5.12 and 4.37 $m^2/g$, when the calcination temperature was increased to 400 ° and 500 °C, respectively.

**Table 5.2** Surface area of the bismuth oxide synthesized at different morphologies and calcination temperatures.

| Morphology | Bismuth oxide | |
|---|---|---|
| | Calcination Temperature (°C) | Surface area ($m^2/g$) |
| Plate-like (B1C300) | 300 | 12.10 |
| Thick wall flower like (B7C300) | 300 | 23.18 |
| Thin wall flower like (B4C300) | 300 | 23.21 |
| Thin wall flower like (B4C400) | 400 | 5.12 |
| Thin wall flower like (B4C500) | 500 | 4.73 |

## 5.5 Conclusions

Flower-like bismuth oxide precursor was successfully synthesized via a facile route by heating the bismuth nitrate salts in an EG solution at 150 °C for 2 h. Triethanolamine catalyzed the reaction at low temperature (100 °C) and significantly affected to nanostructure formation. The flower-like formation involved fast nucleation and growth stages to form nanoplates in which each nanoplate further

assembled itself through self-assembly process. Various morphologies were observed as increasing the metal concentration.

## 5.6 Acknowledgements

This research work is financially supported by the Postgraduate Education and Research Program in Petroleum and Petrochemical Technology (ADB) Fund (Thailand) and the Ratchadapisake Sompote Fund, Chulalongkorn University (Thailand).

## 5.7 References

[1] N.M. Sammes, G.A. Tompsett, H. Näfe, and F. Aldinger, Bismuth based oxide electrolytes-structure and ionic conductivity, Journal of the European Ceramic Society, 19 (1999) 1801-1826.

[2] G.H. Hwang, W.K. Han, J.S. Park, and S.G. Kang, An electrochemical sensor based on the reduction of screen-printed bismuth oxide for the determination of trace lead and cadmium, Sensors and Actuators B. 135 (10) (2008) 309-316.

[3] L. Leontie, M. Caraman, I. Evtodiev, E. Cuculescu, and A. Mija, Optical properties of bismuth oxide thin films prepared by reactive d.c. magnetron sputtering onto p-GaSe (Cu), Physica Status Solidi (a)-Applications and Materials Science, 205 (8) (2008) 2052– 2056.

[4] L. Leontie, M. Caraman, A. Visinoiu, G.I. Rusu, On the optical properties of bismuth oxide thin films prepared by pulsed laser depositon, Thin Solid Films. 473 (2005) 230–235.

[5] S.Y. Chai, Y.J. Kim , M.H. Jung, A.K. Chakraborty, D. Jung, W.I. Lee, Heterojunctioned $BiOCl/Bi_2O_3$, a new visible light photocatalyst, Journal of Catalysis, 262 (2009)144–149.

[6] Y. Xiong, M. Wu, J. Ye, Q. Chen, Synthesis and luminescence properties of hand-like $\alpha$-$Bi_2O_3$ microcrystals, Materials Letters, 62 (2008) 1165-1168.

[7] R. Chen, Z.R. Shen, H. Wang, H.J. Zhou, Y.P. Liu, D.T. Ding, T.H. Chen, Fabrication of mesh-like bismuth oxide single crystalline nanoflakes and their

visible light photocatalytic activity, Journal of Alloys and Compounds, 509 (2011) 2588-2595.

[8] Y. Wang, J. Zhao, Z. Wang, A simple low-temperature fabrication of oblique prism-like bismuth oxide via a one-step aqueous process, Colloids and Surfaces A: Physicochem. Eng. Aspects, 377 (2011) 409-413.

[9] P. Xiao, L. Zhu, Y. Zhu, Y. Qian, Selective hydrothermal synthesis of BiOBr microflowers and $Bi_2O_3$ shuttles with concave surfaces, Journal of Solid State Chemistry, 184 (2011) 1459-1464.

[10] J. Zhu, S. Wang, J. Wang, D. Zhang, H. Li, Highly active and durable $Bi_2O_3/TiO_2$ visible photocatalyst in flower-like spheres with surface-enriched $Bi_2O_3$ quantum dots, Applied Catalysis B: Environmental, 102 (2011) 120-125.

[11] L. Zhang, Y. Hashimoto, T. Taishi, I. Nakamura, Q.Q. Ni, Fabrication of flower-shaped $Bi_2O_3$ superstructure by a facile template-free process, Applied Surface Science, 257 (2011) 6577-6582.

[12] L. Zhou, W. Wang, H. Xu, S. Sun, M. Shang, $Bi_2O_3$ hierarchical nanostructures: Controllable synthesis, growth mechanism, and their application in photocatalysis, Chemistry-A European Journal, 15 (2009) 1776 – 1782.

[13] T.K. Tseng, J. Choi, D.W. Jung, M. Davidson, P.H. Hollyway, Three-dimensional self-assembled hierarchical architectures of gamma-phase flowerlike bismuth oxide, ACS Applied Materials and Interfaces, 2 (4) (2010) 943–946.

[14] J. Geng, F. Wang, Y. Wu, G. Lu, The evidences of morphology dependent electroactivity toward CO oxidation over bismuth oxide supported Pt, Catalysis Letters, 135 (2010) 114–119.

[15] J. Li, H. Fan, J. Chen, L. Liu, Synthesis and characterization of poly(vinyl pyrrolidone)-capped bismuth nanospheres, Colloids and Surfaces A: Physicochem. Eng. Aspects, 340 (2009) 66-69.

[16] R.J. Joseyphus, T. Matsumoto, H. Takahashi, D. Kodama, K. Tohji, B. Jeyadevan, Designed synthesis of cobalt and its alloys by polyol process, Journal of Solid State Chemistry, 180 (2007) 3008-3018.

[17] D. Wang, R. Yu, N. Kumada, N. Kinomura, Hydrothermal synthesis and characterization of a novel one-dimensional titanium glycolate complex single crystal: $Ti(OCH_2CH_2O)_2$, Chemistry of Materials. 11 (1999) 2008-2012.

[18] R.P. Oertel, R.A. Plane, Raman and infrared study of nitrate complexes of bismuth (III), Inorganic Chemistry, 7(6) (1968) 1192.

[19] T. Zevaco, M. Postel, Bismuth (III) Complexes from Glycol and α-Hydroxycarboxylic acid, Synthesis and Reactivity in Inorganic and Metal-Organic Chemistry, 22 (2&3) (1992) 289-297.

[20] D. Larcher, G. Sudant, R. Patrice, J.-M. Tarascon, Some insights on the use of polyols-based metal alkoxides powders as precursors for tailored metal-oxides particles, Chemistry of Materials, 15 (2003) 3543-3551.

[21] N. Chakroune, G. Viau, S. Ammar, N. Jouini, P. Gredin, M.J.Vaulay, F. Fievet, Synthesis, characterization and magnetic properties of disk-shaped particles of a cobalt alkoxide: $Co^{II}(C_2H_4O_2)$, New journal of Chemistry, 29 (2005) 355-361.

[22] D. Larcher, B. Gerand, J.M. Tarascon, Synthesis and electrochemical performances of $Li_{1+y}Mn_{2-y}O_4$ powders of well-defined morphology, Journal of Solid State Chemistry, 2 (1998) 137-145.

[23] F. Fievet, J.P. Lagier, B. Blin, B. Beaudoin, M. Figlarz, Homogeneous and Heterogeneous nucleations in the polyol process for the preparation of micron and submicron size metal particle, Solid State Ionics. 32/33 (1989) 198-205.

[24] B.F. Bonet, C. Gue´ry, D. Guyomard, R. Herrera Urbina, K. Tekaia-Elhsisen, J.-M. Tarascon, Electrochemical reduction of noble metal compounds in ethylene glycol, International Journal of Inorganic Materials, 1 (1999) 47–51.

[25] X.Y. Liu, J.H. Zeng, S.Y. Zhang, R.B. Zheng, X.M. Liu, Y.T. Qian, Novel bismuth nanotube arrays synthesized by solvothermal method, Chemical Physics Letters, 374 (2003) 348–352.

[26] C. Goia, E. Matijevic´, D.V. Goia, Preparation of colloidal bismuth particles in polyols, Journal of Materials Research, 20(6) (2005) 1507-1514.

[27] F. Li, J. Wu, Q. Qin, Z. Li, X. Huang, Controllable synthesis, optical and photocatalytic properties of CuS nanomaterials with hierarchical structures, Powder Technology, 198 (2010) 267-274.

[28] M.G.Ma, J.F.Zhu, R.C. Sun, Y.J. Zhu, Microwave-assisted synthesis of hierarchical $Bi_2O_3$ spheres assembled from nanosheets with pore structure, Materials Letters, 64 (2010) 1524-1527.

[29] L.S. Zhong, J.S. Hu, H.P. Liang, A.M. Cao, W.G. Song, L.J. Wan, Self-Assembled 3D Flowerlike Iron Oxide Nanostructures and their application in Water Treatment, Advanced Materials, 18 (2006) 2426–2431.

[30] J. Yang, C. Li, Z. Quan, C. Zhang, P. Yang, Y. Li, C. Yu, J. Lin, Self-assembled 3D flowerlike $Lu_2O_3$ and $Lu_2O_3$:$Ln^{3+}$ (Ln = Eu, Tb, Dy, Pr, Sm, Er, Ho, Tm) Microarchitectures: ethylene glycol-mediated hydrothermal synthesis and luminescent properties, Journal of Physical Chemistry C, 112 (33) ( 2008) 12777–12785.

[31] A.M. Cao, J.S. Hu, H.P. Liang, W.G. Song, L.J. Wan, X.L. He, X.G. Gao, S.H. Xia, Self-Assembled 3D Flowerlike $Lu_2O_3$ and $Lu_2O_3$:$Ln^{3+}$ (Ln = Eu, Tb, Dy, Pr, Sm, Er, Ho, Tm) Microarchitectures: Ethylene Glycol-Mediated Hydrothermal Synthesis and Luminescent Properties, Journal of Physical Chemistry B, 110 (2006) 15858-15863.

[32] Y. Wang, S. Li, X. Xing, F. Huang, Y. Shem, A. Xie, X. Wang, J. Zhang, Self-assembled 3D flower-like hierarchical $Fe_2O_3$@$Bi_2O_3$ core-shell architecture and their enhanced photocatalytic activity under visible light, Chemistry-A European Journal , 7 (2011) 4802-4808.

[33] B. Yang, M. Mo, H. Hu, C. Li, X. Yang, Q. Li, Y. Qian, A rational self-sacrificing template route to β-$Bi_2O_3$ nanotube arrays, European Journal of Inorganic Chemistry, 9 (2004) 1785–1787.

[34] X. Jiang, Y. Wang, T. Hericks, Y. Xia, Ethylene glycol-mediated synthesis of metal oxide nanowires, Journal of Materials Chemistry, 14 (2004) 695-703.

[35] O. Monnereau, L. Tortet, P. Llewellyn, F. Rouquerol, G. Vacquier, Synthesis of $Bi_2O_3$ by controlled transformation rate thermal analysis: a new route for this oxide?, Solid State Ionics. 157 (2003) 163– 169.